

Supporting Information

Antibody-Armed Platelets for Regenerative Targeting of Endogenous Stem Cells

*Deliang Shen,^{1,2,3,‡} Zhenhua Li, ^{*2,3,4,‡} Shiqi Hu,^{2,3,‡} Ke Huang,^{2,3} Teng Su,^{2,3}*

*Hongxia Liang,^{1,2,3} Feiran Liu,^{2,3} and Ke Cheng^{*2,3}*

¹Department of Cardiology, The First Affiliated Hospital of Zhengzhou

University, Zhengzhou, Henan 450052, China

²Department of Molecular Biomedical Sciences and Comparative Medicine

Institute, North Carolina State University, Raleigh, North Carolina 27607, United States

³Joint Department of Biomedical Engineering, University of North Carolina at

Chapel Hill and North Carolina State University, Raleigh, North Carolina 27695,

United States

⁴College of Chemistry & Environmental Science, Hebei University, Baoding

071002, China

‡These authors contributed equally.

*E-mail: kcheng3@ncsu.edu; Phone: +1-919-513-6157 or

zhenhuali@hbu.edu.cn; Phone: +86-13331210907

Materials

CD34 antibodies were purchased from Santa Cruz. DSPE-PEG-NHS (MW5K) was obtained from NANOCS. Mouse IgG total ELISA Kit was obtained from Fisher Scientific. C57BL/6 mouse bone marrow endothelial progenitor cells (EPC) and complete mouse endothelial cell medium /w Kit were obtained from Cell Biologics. GFP-tagged HUVECs were obtained from Angio-Proteomie. Anti-mouse Ki67, vWF, CD8, and CD68 antibodies were purchased from Abcam. Goat anti-mouse and anti-rabbit IgG Secondary Antibody, and Alexa Fluor 488 and 594 were obtained from Invitrogen. Trichrome Stain (Masson) Kit and Anti-Mouse IgG (whole molecule) - Gold antibody produced in goat were purchased from Sigma-Aldrich. Endothelial cell growth Kit-VEGF and vascular cell basal medium were obtained from ATCC. Mouse IgG whole molecule was purchased from Jackson ImmunoResearch Inc.

Isolation of platelets

Murine platelets were isolated as previously described.¹ In brief, whole blood was collected from the C57BL/6 mice (non-terminal collection from the orbital sinus or saphenous vein; 20 mice were used) into a plastic syringe containing 1.0 mL citrate-phosphatedextrose (16 mM citric acid, 90 mM sodium citrate, 16 mM NaH₂PO₄, 142 mM dextrose, pH 7.4) and centrifuged at 100 g for 20 min at room temperature. The platelet-rich plasma (PRP) was transferred to a separate tube using a transfer pipette (wide orifice), and PGE1 was added to each tube at a final concentration of 1 μM. Platelets were isolated from the PRP via centrifugation at 800 g for 10 min. The plasma was discarded, and the platelets were resuspended carefully in Tyrode's buffer (134 mM NaCl, 12 mM NaHCO₃, 2.9 mM KCl, 0.34 mM Na₂HPO₄, 1 mM MgCl₂, 10 mM HEPES, pH 7.4) or PBS with PGE1 added at 1 μM.

Linking of CD34 antibodies to DSPE-PEG-NHS

CD34 antibodies were first reacted with DSPE-PEG-NHS by -NH₂ and NHS acylation

reactions. Equimolar CD34 antibodies and DSPE-PEG-NHS were mixed together and reacted at 4°C for 24 h. Then the unreacted DSPE-PEG-NHS was removed by centrifugation using Amicon Ultra-0.5 Filter (100kDa). Successful conjugation was confirmed by SDS-PAGE.

Conjugation of CD34 antibodies onto platelets (P-CD34)

DSPE can bind with the membranes of cells, liposomes, and platelets. The surface of the platelets was functionalized with CD34 antibodies by DSPE-PEG-CD34. 10^8 platelets were dispersed in PBS buffer and then DSPE-PEG-CD34 with different concentrations was added. The mixture was stirred for 3 h and then unconjugated DSPE-PEG-CD34 was removed by centrifugation at 800 g for 10 min. The P-CD34 was then washed twice using centrifugation at 800 g for 10 min.

Quantify the number of CD34 on platelets

P-CD34 was resuspended in 100 μ L of deionized water and ultrasonicated to lyse the platelets and release the DSPE-PEG-CD34. The amount of CD34 conjugated to the platelets was measured using ELISA.

Confirmation of the presence of CD34 antibodies on platelets

P-CD34 were incubated with gold nanoparticles-labeled goat anti-mouse IgG (10 nm) and FITC-labeled goat anti-mouse IgG, respectively, for 2 h, at room temperature. The free IgG antibodies were removed by centrifugation at 800 g for 10 min. The prepared samples were observed using TEM and fluorescence microscopy.

EPC capturing assay

EPCs were first cultured on 4-well slides and then stained using DiI. Then DiO-labeled platelets, P-IgG, and P-CD34 were co-cultured with EPCs for 6 h. After incubation, the cells were washed three times with PBS and counter-stained with DAPI for another 15 min. Imaging was performed using a Nikon Fluorescent Microscope. The binding ratio between platelet and

EPC was calculated then. We first cultured 5×10^4 EPCs in 96 well plate. After the cells attached to the plate, the culture medium was removed and washed with PBS for 3 times to avoid their proliferation. Then excess platelets (5×10^6) were added to every well and incubated for another 1 h. The unattached platelets in culture supernatant were counted by haemocytometer. The binding ratio (BR) can be calculated by the formula:

$$BR = \frac{\text{Number of platelet in stock solution} - \text{Number of platelet in supernatant}}{\text{Number of cells}}$$

Collagen surface binding assay

GFP-tagged HUVECs were seeded on collagen-coated (Sigma Aldrich) 4-well culture chamber slides (Thermo Fisher Scientific) and cultured in Vascular Cell Basal Medium™ supplemented with endothelial cell growth kit-VEGF™. EPCs were first pre-treated using platelets, P-IgG, and P-CD34. The EPCs were then centrifuged to remove unattached platelets, P-IgG, and P-CD34. The slides were then incubated with DiI-labeled EPCs pretreated with platelets, P-IgG, and P-CD34 in PBS at 4°C for 5 min. Next, the cells were washed with PBS twice and imaged using Fluorescence Microscopy. Attached EPCs were quantified.

Denuded rat aorta binding assay

To examine the binding of P-CD34 pre-treated EPCs (P-EPC) and non-treated EPCs onto injured (denuded) vascular walls, aortas from C57BL/6 mice were dissected and surgically scraped on their luminal side with forceps, to remove the endothelial layer. Successful denudation was confirmed by microscopy visualization. Both denuded or control aortas were incubated with DiI-labeled P-EPC or EPCs for 5 min. After PBS rinses, the samples were subjected to fluorescence microscopy examination for cell binding.

Cardiomyocyte proliferation assay

NRCMs were derived from SD rats as previously described.² NRCM were cultured on four-well

chamber slides for 3 d, followed by co-incubation with P-CD34 or conditioned medium from P-CD34 pretreated EPCs for 24 h. After that, the cells were washed with PBS twice, fixed, permeabilized, and stained for Ki67, followed by DAPI staining for nucleus visualization. Images were taken using a Zeiss LSM 710 confocal microscope (Carl Zeiss, Germany).

EPCs capturing ability of P-CD34 in whole blood

Whole blood was collected from C57BL/6 mice. EPCs (10^5) were then stained using DiI and mixed with 1 mL of whole blood. DiO-labeled platelets, P-IgG, and P-CD34 were added and incubated for 30 min. Then the RBCs were lysed, and the samples were analyzed using flow cytometry.

Aggregation assay

To determine if P-CD34 induced any adverse pro-thrombotic effects, 450 μ L of platelet poor plasma (PPP) was collected and added to glass cuvettes for aggregometry. Aggregometry was performed using a commercial optical (light transmission) aggregometer (Chrono-log 700 manual, Chrono-log Corp.) with the addition of collagen (10 μ g/mL) as the platelet agonist. The following analyses were performed: (1) freshly prepared platelets; (2) platelets that were isolated and stored for 1 day at 4°C; (3) P-CD34 processed from platelets under Condition (2).

Mouse model of myocardial infarction

All animal work was compliant with the Institutional Animal Care and Use Committee (IACUC) of the University of North Carolina at Chapel Hill and North Carolina State University. Briefly, female C57BL/6 mice (8–10 weeks old, Charles River Laboratories) were anesthetized by inhalation of 3% isoflurane in 100% oxygen at a flow rate of 2 L·min⁻¹. Under sterile condition, the heart was exposed by a left thoracotomy and ischemia was achieved by permanent ligation of the left anterior descending coronary artery. 3 mice were randomly selected from the MI or the non-MI group for triphenyltetrazolium chloride (TTC) staining to

evaluate the homogeneity of the MI model. Infarction (%) was calculated as $IA/LV \times 100$ (IA is the infarct area while LV is the total area of left ventricle). About 30 min later the G-CSF was administered, and the drugs were given for another 2 days (once per day). The blood were draw and analyzed using a Mouse Cytokine Antibody Array (MOUSE CYTOKINE ARRAY C3 (4), Raybiotech Inc), which can detect 62 mouse cytokines simultaneously. After that, animals were randomized into four treatment groups (n = 9 mice per group): 1) i.v. injection of 100 μ L PBS; 2) i.v. injection of 10^8 bare platelets in 100 μ L PBS; 3) P-IgG; and 4) P-CD34. For CD34-positive cells recruitment assessment, 3 of 9 mice were euthanatized and the hearts was harvested 3 days after. The rest 6 animals were sacrificed 4 weeks after injection for histological analysis. We also evaluated the capturing efficiency of P-CD34 *in vivo*. P-IgG and P-CD34 were intravenously injected after G-CSF treatment. 6 h post injection, blood was taken to measure the binding of P-CD34 to CD34+ cells using flow cytometry. The capturing efficiency (CE) could be calculated from the following equation:

$$CE = \frac{\text{double positive \%}}{\text{double positive \%} + \text{anti - CD34 positive \%}} * 100\%$$

In addition, hearts were cryo-sectioned at 10 μ m thickness from the apex to the ligation level with 100 μ m intervals for immunohistochemistry.

Cardiac function assessment

The transthoracic echocardiography procedure was performed by a cardiologist who was blinded for animal group allocation using a Philips CX30 ultrasound system coupled with a L15 high-frequency probe. All animals inhaled a 1.5% isoflurane-oxygen anesthesia mixture in supine position at the 4-hr and 4-week time points (n = 6 mice per group). Hearts were imaged 2D in long-axis views at the level of the greatest left ventricular (LV) diameter. LV end-diastolic volume (LVEDV) and LV end-systolic volume (LVESV) were measured. Ejection fraction (EF) was determined by measurements from views taken from the infarcted area. Left

ventricular end-systolic dimension (LVDs), end-diastolic dimension (LVDd) and fractional shortening (LVFS) were calculated in each echocardiogram.

Platelets targeting to MI area

To confirm the MI-targeting ability of P-CD34, DiR- or DiO-labeled P-CD34 were i.v. injected after MI. DiR-labeled groups was detected using IVIS imaging system at different time interval.

The DiO-labeled group was used for immunohistochemistry assessment.

Heart morphometry

After the echocardiography study at 4 weeks, animals were euthanized and hearts were harvested and frozen in OCT compound. Specimens were sectioned at 10 μ m thickness from the apex to the ligation level with 100 μ m intervals. Masson's trichrome staining was performed as described by the manufacturer's instructions. Images were acquired with a PathScan Enabler IV slide scanner (Advanced Imaging Concepts, Princeton, NJ). From the Masson's trichrome stained images, morphometric parameters, including viable myocardium, scar size, and infarct thickness were measured in each section with NIH ImageJ software. The percentage of viable myocardium as a fraction of the scar area (infarcted size) was quantified. Three selected sections were quantified for each animal.

Immunohistochemistry assessment

Heart cryosections were fixed with 4% paraformaldehyde in PBS for 30 min, permeabilized, and blocked with Protein Block Solution (DAKO) containing 0.1% saponin for 1 h, at room temperature. For immunostaining, the samples were incubated overnight at 4 °C with the following primary antibodies diluted in the blocking solution: rabbit anti-mouse alpha sarcomeric actin (1:200, ab137346, Abcam) was used to identify cardiomyocytes; rat anti-mouse Ki67 antibody (1:200, 151202, Biolegend) was used to analyze cell-cycle re-entry; sheep anti-mouse vWF antibody (1:200, ab11713, Abcam) was used to detect myocardial

capillaries in the peri-infarct regions; rat anti-mouse CD34 antibody (1:200, MA1-22646, Thermo Fisher Scientific) was used to examine endogenous progenitor/stem cell recruitment; rat anti-mouse CD8 (1:200, ab22378, Abcam), and rabbit anti-mouse CD68 (1:200, ab125212, Abcam) antibody was used to detect immune response. After three 10-min washes with PBS, samples were stained for 1.5 h at room temperature with fluorescent secondary antibodies, including goat anti-rabbit IgG-Alexa Fluor 594 conjugate (1:400, ab150080, Abcam), goat anti-rat IgG-Alexa Fluor 488 conjugate (1:400, ab150157, Abcam), goat anti-rabbit IgG-Alexa Fluor 488 conjugate (1:400, ab150077, Abcam), and goat anti-rabbit IgG-Alexa Fluor 594 conjugate (1:400, ab150080, Abcam) based on the isotopes of the primary antibodies. This was followed by 10 min of 4, 6-diamidino-2-phenylindole dihydrochloride (DAPI) staining for nucleus visualization. Slides were mounted with ProLong Gold mountant (Thermo Fisher Scientific) and viewed using an Olympus epi-fluorescence microscopy system. Four slides were stained for each group and 4 randomly selected fields from each slide ($n = 4$) were analyzed with the NIH ImageJ software. The red, green, and blue channels were split (RGB), and integrated densities of green signal were calculated using the software.

Statistical analysis

All experiments were performed independently at least three times, and the results were presented as mean \pm s.d. Comparisons between any two groups were performed using two-tailed, unpaired Student's *t*-test. Comparisons among more than two groups were performed using one-way ANOVA, followed by post hoc Bonferroni test. Single, double, and triple asterisks represent $p < 0.05$, 0.01, and 0.001, respectively; $p < 0.05$ was considered statistically significant.

Reference

(1) Tang, J.; Su, T.; Huang, K.; Dinh, P.-U.; Wang, Z.; Vandergriff, A.; Hensley, M. T.; Cores, J.; Allen, T.; Li, T.; Sproul, E.; Mihalko, E.; Lobo, L. J.; Ruterbories, L.; Lynch, A.; Brown, A.; Caranasos, T. G.; Shen, D.; Stouffer, G. A.; Gu, Z.; Zhang, J.; Cheng, K. *Nat. Biomed. Eng.* **2018**, *2*, 17—26.

(2) Su, T.; Huang, K.; Ma, H.; Liang, H.; Dinh, P.-U.; Chen, J.; Shen, D.; Allen, T. A.; Qiao, L.; Li, Z.; Hu, S.; Cores, J.; Frame, B. N.; Young, A. T.; Yin, Q.; Liu, J.; Qian, L.; Caranasos, T. G.; Brudno, Y.; Ligler, F. S.; Cheng, K. *Adv. Funct. Mater.* **2018**, 1803567.

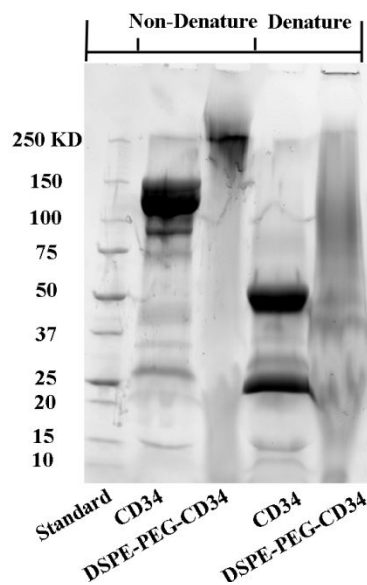


Figure S1. SDS-PAGE analysis. Left to right: Ladders, CD-34 (Non-Denaturing), CD34-DSPE (Non-Denaturing), CD34 (Denaturing), CD34-DSPE (Denaturing).

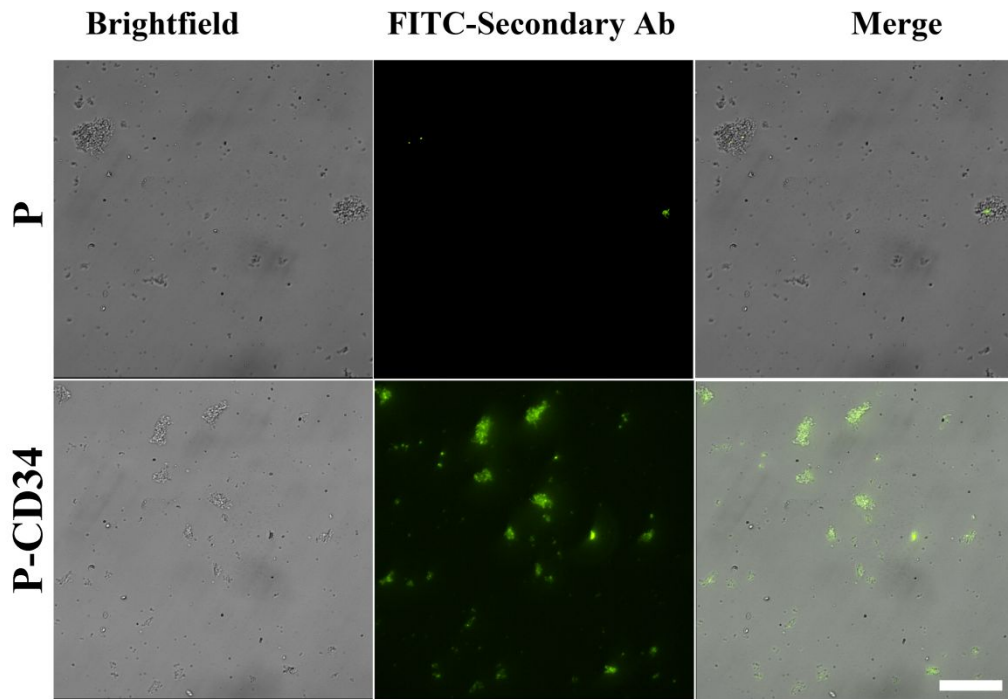


Figure S2. Attachment of CD34 antibodies on platelets. P-CD34s were detected by FITC-labeled secondary antibodies. Scale bar, 10 μm .

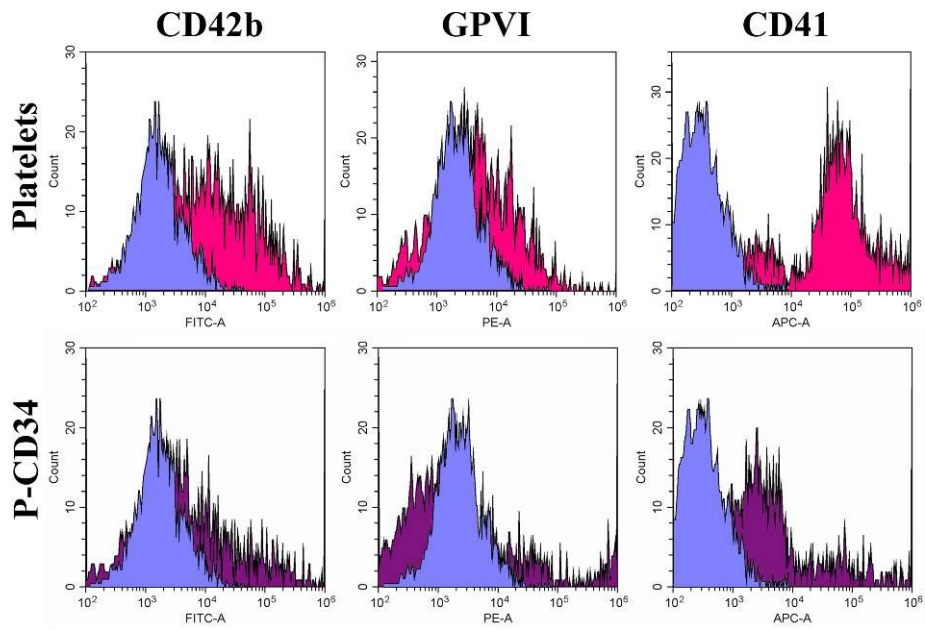


Figure S3. Surface marker expression on native and CD34-conjugated platelets (P-CD34).

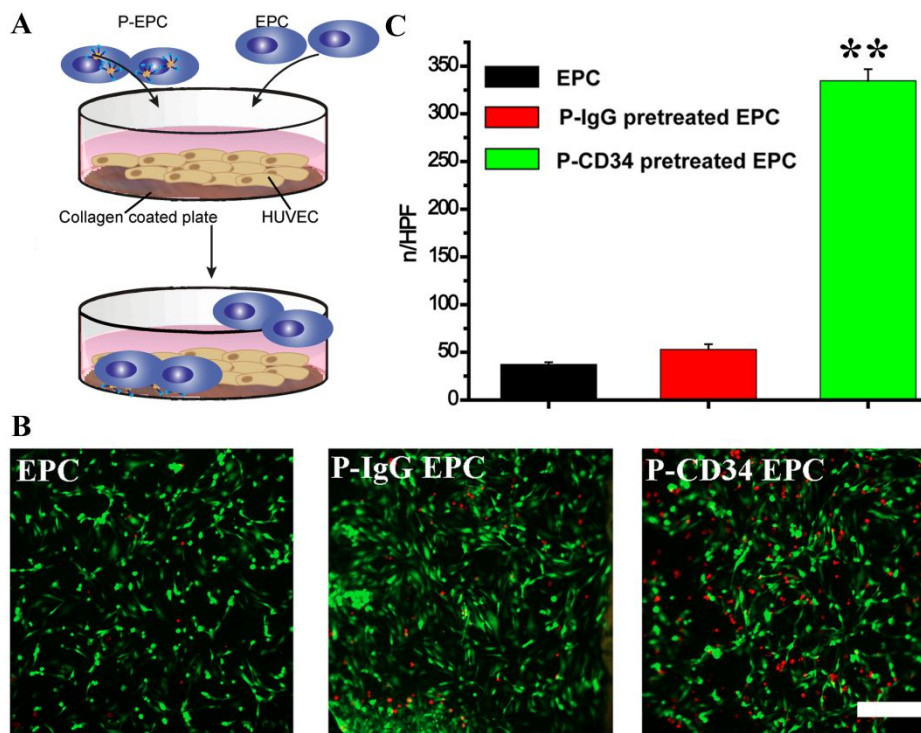


Figure S4. Platelets help EPC bind to collagen. (A) Schematic showing the experimental design. (B) Representative fluorescent images showing the binding of DiI-labelled EPCs, P-IgG pretreated EPCs, or P-CD34 pretreated EPCs on collagen surfaces (seed with HUVECs). (C) Quantitative analysis of cell binding to collagen. $n=4$ for each group. All data are mean \pm s.d. Scale bar = 100 μm . ** $P < 0.01$.

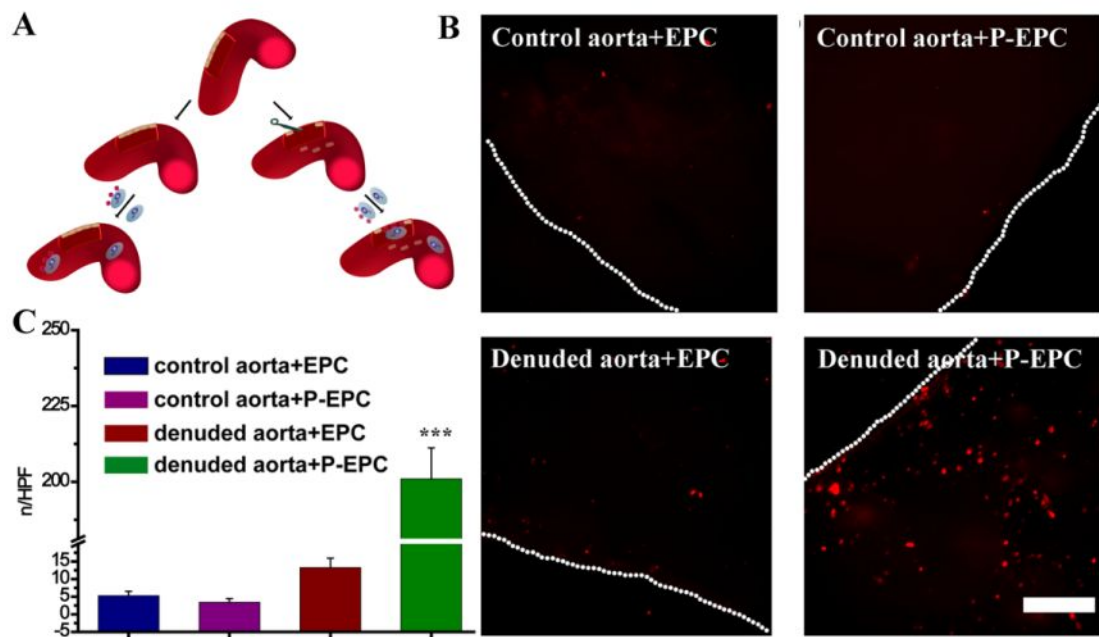


Figure S5. Platelets promote EPC binding to damaged vasculatures. (A) Augmented binding of P-CD34-decorated EPC (P-EPC) to damaged rodent vasculatures. (B) Representative fluorescent micrographs showing the adhesion of DiI-labelled P-EPCs or EPCs on control or denuded aortas. (C) Quantitative analysis of cell binding to denuded aorta. n=4 for each group. All data are mean \pm s.d. Scale bar = 100 μ m, ***P < 0.005.

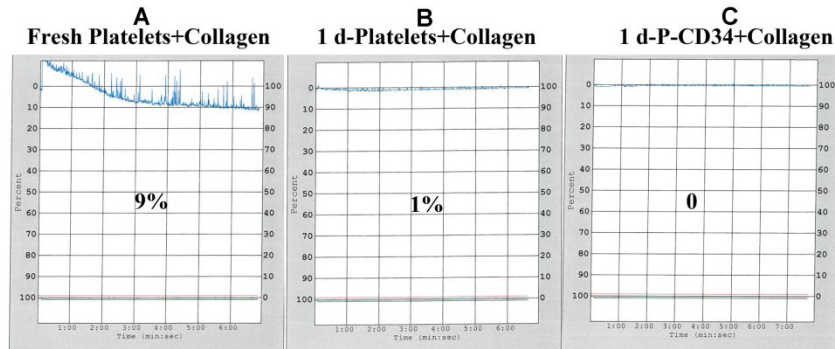


Figure S6. Aggregometry assay. Aggregometry was performed on platelet poor plasma (PPP) mixed with freshly prepared platelets (A), platelets stored for 1 day at 4°C (B), or P-CD34 processed from platelets under Condition (B) in the presence of collagen.

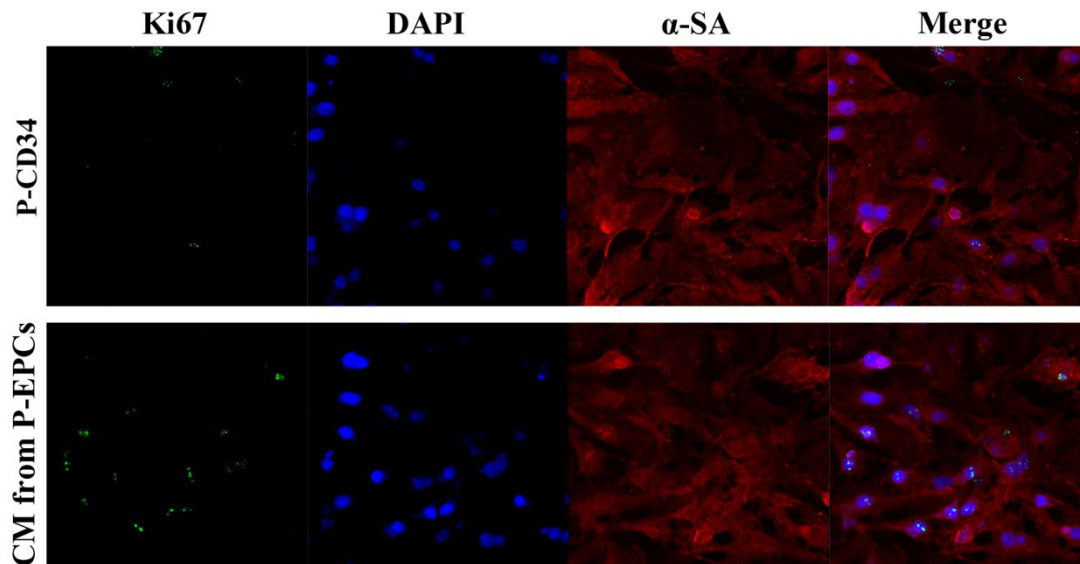


Figure S7. The proliferation of NRCM cells in the presence of P-CD34 alone or CM from P-CD34 attached EPCs.

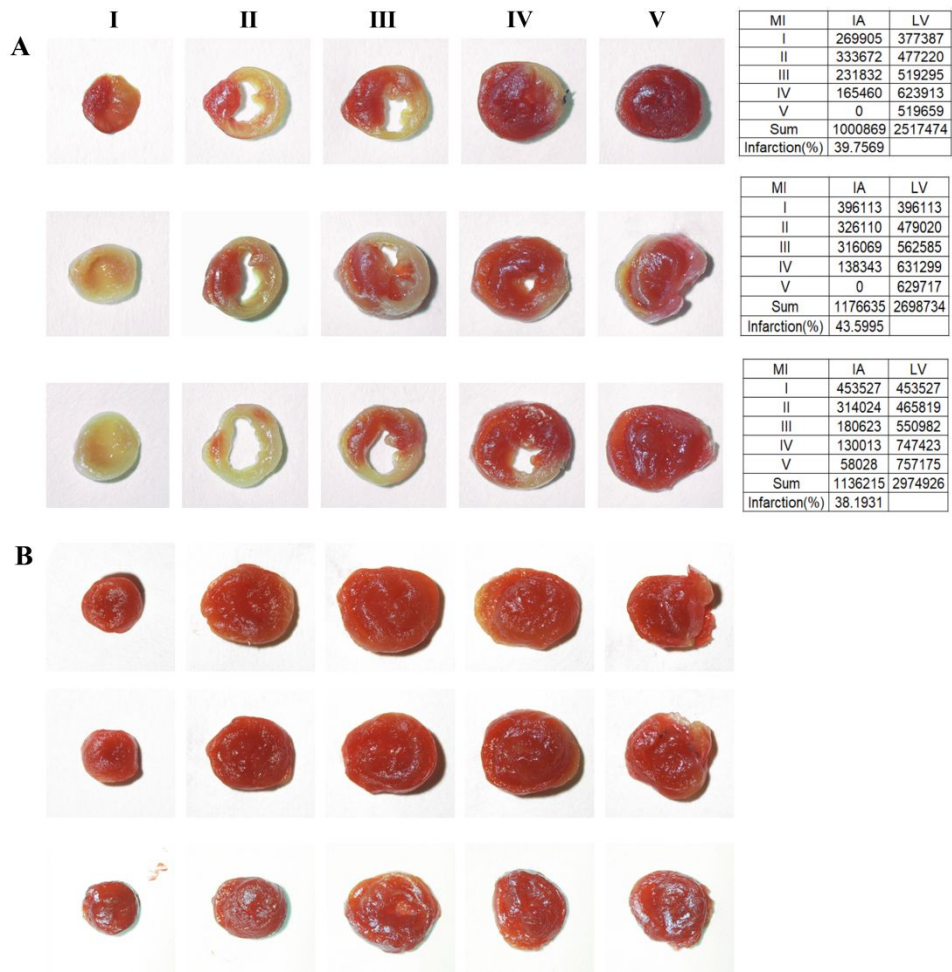


Figure S8. Representative TTC staining images of MI mice (A) and sham mice (B). The grey area indicates infarct region and the red area indicates viable myocardium.

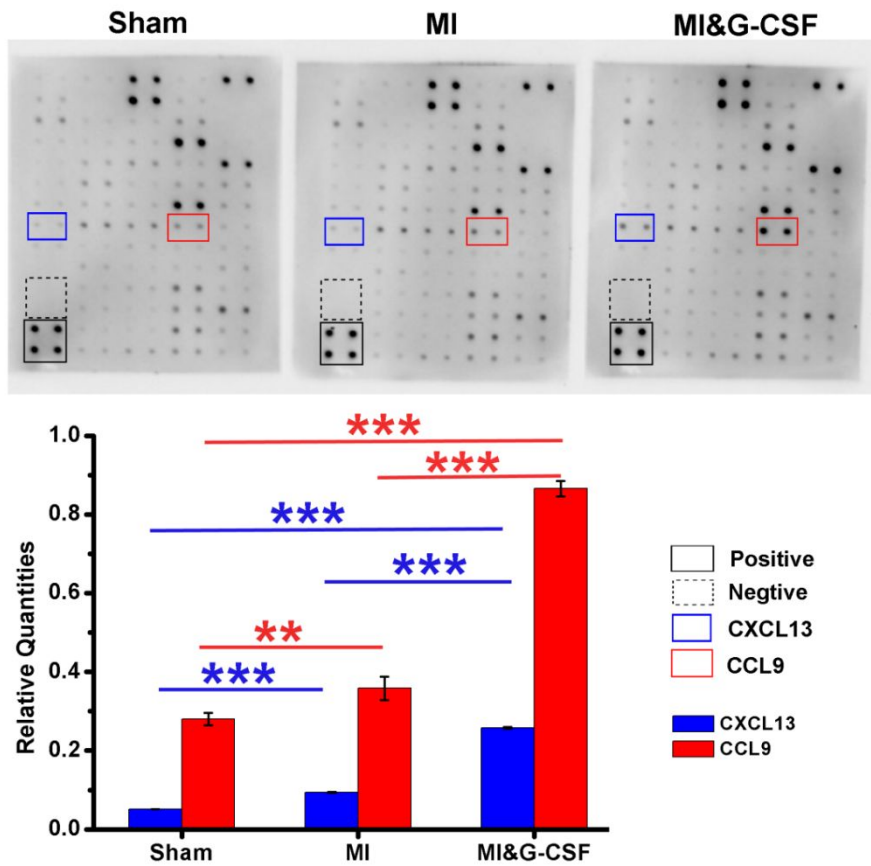


Figure S9. Cytokine array analysis of systemic inflammatory cytokine levels after G-CSF stimulation (n = 3 animals per group).

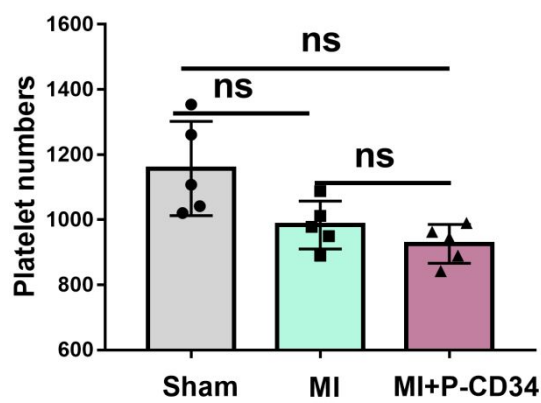


Figure S10. The numbers of platelets in the blood (n = 6 animals per group).

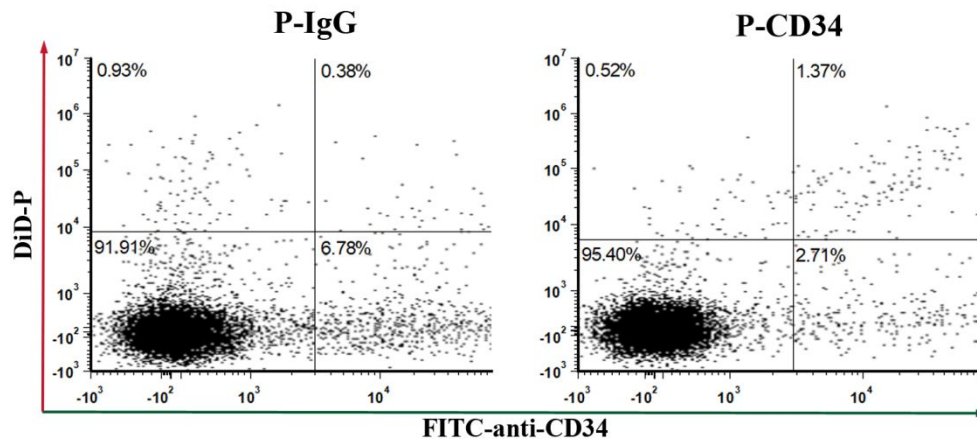


Figure S11. Flow cytometry analysis showing the ability of P-CD34 to capture EPCs *in vivo*.

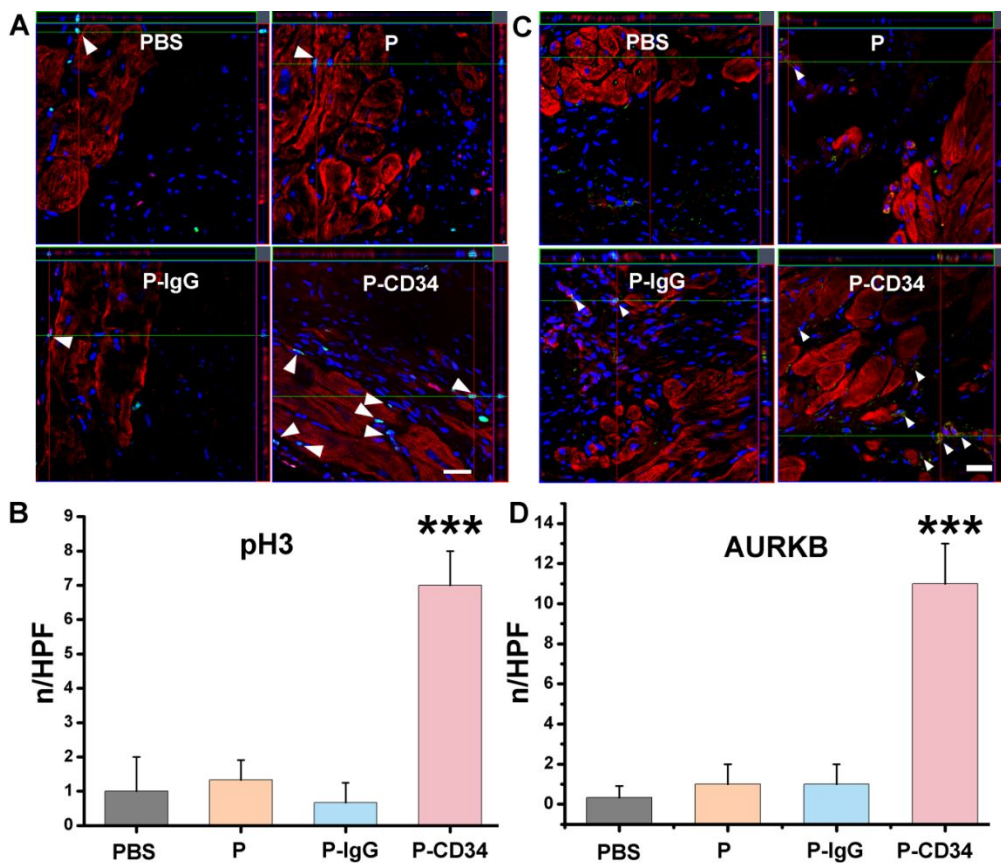


Figure S12. Z-stack analysis of mitotic activities of cardiomyocytes. (A) Representative confocal images showing phospho-histone H3 (pH3)-positive nuclei in cardiomyocytes (white arrowheads) in the peri-infarct regions of PBS-, platelets-, P-IgG-, or P-CD34-treated hearts 4

weeks after the therapy. (B) Quantitative analysis of pH3-positive cardiomyocytes. (C) Visualization of AURKB-positive nuclei in cardiomyocytes (white arrowheads) in the peri-infarct regions. (D) Quantitative analysis of AURKB-positive cardiomyocytes. Scale bars, 20 μ m. P-CD34 groups vs other groups, *** indicates $p < 0.001$.

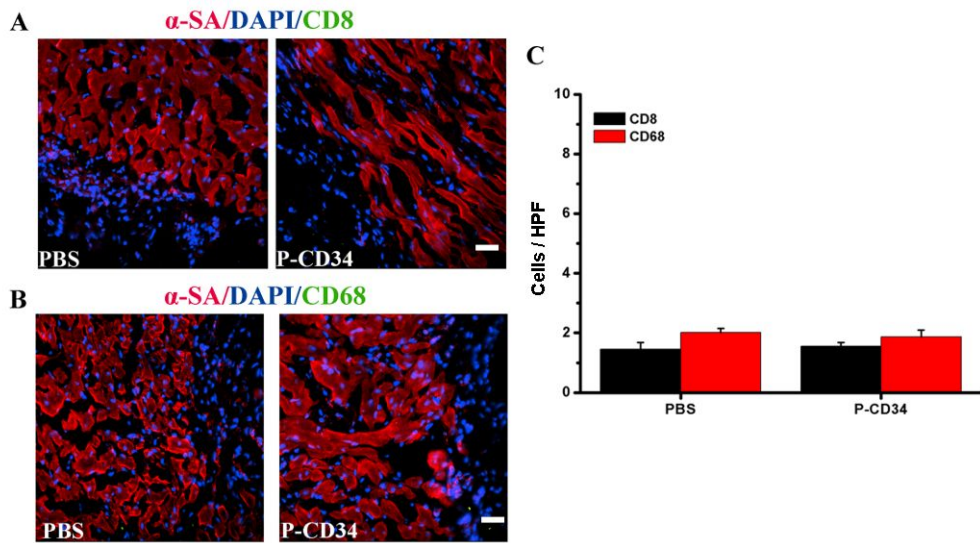


Figure S13. Immune response to P-CD34 injections. (A) Microscopic images showing CD8-positive T cells and (B) CD68-positive macrophages (magenta) in the infarct area. (C) Quantitative analysis results. (n = 4 images per slides). Scale bars, 20 μ m.

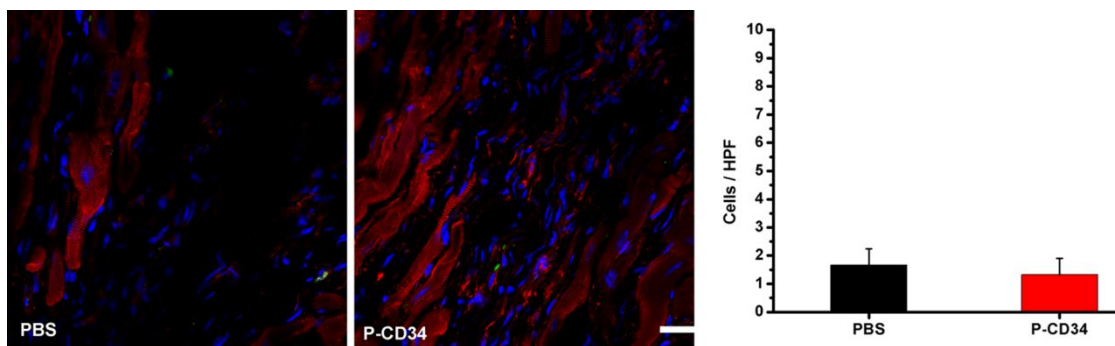


Figure S14. F4/80-positive macrophages in the infarct area. Scale bars, 20 μ m.